Passage through resonance and autoresonance in x^{2n}-type potentials

E. Nakar and L. Friedland
Racah Institute of Physics, Hebrew University of Jerusalem, 91904 Jerusalem, Israel
(Received 7 June 1999)

Resonant dynamics of a particle in an x^{2n}-type potential driven by an oscillation with adiabatically varying frequency is investigated. It is shown that, under certain conditions, when the driving frequency increases in time and passes the resonance with the unperturbed system, the oscillator phase locks to the drive and, later, this phase locking is sustained, i.e., the system remains in autoresonance. The initial phase locking by passage through resonance is the main ingredient of the transition to autoresonance and comprises the generalization of previous results for nearly parabolic potentials. [S1063-651X(99)16911-3]

PACS number(s): 05.45.Xt

I. INTRODUCTION

Autoresonance (or self-sustained resonance) is a phenomenon taking place when a resonantly driven nonlinear system stays phase locked with adiabatically varying perturbing oscillation (the drive) even if the drive's frequency (or another system parameter) varies in time. Autoresonance is used in relativistic particle accelerators [1] and other applications, such as, in atomic and molecular physics [2], nonlinear dynamics [3], nonlinear waves [4], fluid dynamics [5], and plasma physics [6]. There exist two scenarios for exciting autoresonance in the system. The first is applying a driving perturbation with initial frequency and phase *tuned* close to those of the unperturbed nonlinear oscillator, which may or may not be excited initially [2]. In this case, at certain conditions, the oscillator remains in resonance (stays phase locked) at later times, as the driving frequency varies in time. Alternatively [7], one can start *out of resonance* and slowly pass the resonant point by chirping the driving frequency. Then, there exists a sharp threshold on the drive's amplitude [5] beyond which the oscillator *automatically* phase locks with the drive and evolves in autoresonance at later times if the variation of the driving frequency continues. The second autoresonant excitation scheme is preferable in practical implementations, since it does not require fine initial tuning. We shall refer to this scheme as *locking by passage through resonance* or LPTR. The theory of LPTR and the aforementioned threshold prediction exist for the case, when one proceeds near the equilibrium position (say $x=0$) of the nonlinear oscillator, and, locally, the confining potential has a nearly parabolic form $V\propto x^2$ [5]. In contrast, in the present work, we shall develop the LPTR theory for oscillators having a nonparabolic form ($V\propto x^{2n}, n>1$) near the equilibrium. This family of potentials comprises a model describing transition to a square potential well as $n\to\infty$. We shall also generalize the LPTR theory to studying the phase locking (with the drive) of initially excited oscillators, and discuss the advanced autoresonance stage in these systems.

Our presentation will be as follows. In Sec. II we shall study the LPTR of a particle for $V\propto x^4$ case in detail. The subsequent autoresonant evolution in this case will be studied in Sec. III. Finally, in Sec. IV we shall generalize to the $n>2$ case and present our conclusions.

II. PHASE LOCKING BY PASSAGE THROUGH RESONANCE

Consider a driven oscillator described by the Hamiltonian

$$H(p,x,t)=\frac{1}{2}p^2+\frac{1}{2n}x^{2n}-\varepsilon x\cos\varphi(t), \tag{1}$$

where n may have values 2,3, . . . , while the last term is a perturbation ($\epsilon\ll 1$) characterized by frequency $\omega(t)=d\varphi/dt$, which is a slowly increasing function of time. For simplicity, we shall assume that this time dependence is linear, i.e., $\omega(t)=\omega_0+\alpha t$ and that all dependent and independent variables (p,x,t) and parameters $(\varepsilon,\ \omega)$ are dimensionless. We shall also assume that the oscillator is excited initially (at $t=t_0$) and study the possibility of phase locking via passage through resonance (LPTR) between the drive and the oscillator and subsequent evolution of the system at later times, $t>t_0$. A typical example illustrating LPTR and the autoresonance in this system is presented in Fig. 1(a), where we show the phase space portrait of the solution of

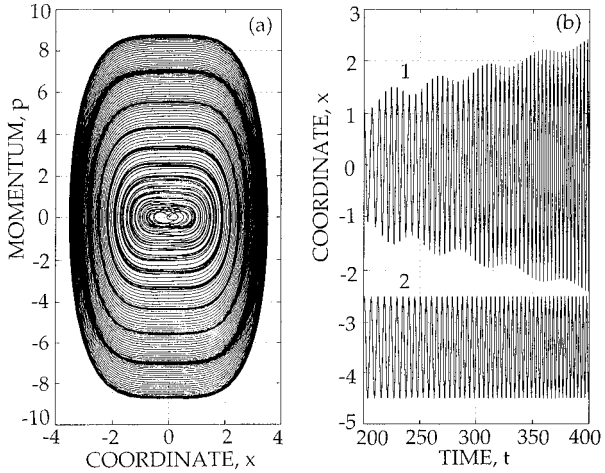

FIG. 1. Autoresonance in the $V=\frac{1}{4}x^4$ potential well. (a) The spiralling phase-space portrait of autoresonant evolution; (b) The coordinate versus time (curve 1) and the function $\cos\varphi(t)-3.5$ (curve 2) representing the driving oscillation. Comparison between the curves illustrates the persisting phase locking in the system despite variation of the driving frequency.

Hamilton's equations $dp/dt=-x^{2n-1}+\ \varepsilon\cos\varphi$, $dx/dt=p$ in the case $n=2$. We used parameters $\epsilon=0.11$, $\alpha=0.005$, $\omega_0=0$, (i.e., $\varphi=\frac{1}{2}\alpha t^2$) and initial conditions $x=0$, $p=0.372$ (at $t=10$) in these calculations. Additional information from the calculations is presented in Fig. 1(b), where we see a part of the evolution of x (curve 1) in the time interval $200<t<400$, as well as the function $\{\cos[\varphi(t)]-3.5\}$ (curve 2 in the figure) representing the shifted (by -3.5) driving perturbation. The phase space portrait in Fig. 1(a) exhibits a spiralling evolution with a slowly increasing averaged energy, while the comparison between the curves in Fig. 1(b) illustrates the phase locking between the solution and the drive despite the variation of the driving frequency. We can also see that the amplitude of these oscillations grows on the average, but also performs slow oscillations around the average. The interference-type pattern in Fig. 1(a) is due to these amplitude oscillations. Our goal is to discuss all stages of evolution in Figs. 1(a) and 1(b) and find the conditions for trapping into resonance and subsequent autoresonance in the system.

The most convenient description of the resonant dynamics in our system is obtained by transforming to action angle variables I and θ associated with the unperturbed problem described by Hamiltonian $H_0=\frac{1}{2}p^2+1/2nx^{2n}$. In this case, $H_0=b_nI^{2n/(n+1)}$, where [8]

$$b_n=(2n)^{-1/(n+1)}\left[\sqrt{\pi/2}(1+n)\frac{\Gamma(1/2+1/2n)}{\Gamma(1/2n)}\right]^{2n/(n+1)}.$$

Then, by expanding $x=\Sigma 2a_k(I)\cos(k\theta)$, we replace the original Hamiltonian by

$$H'=H_0(I)-\epsilon\sum\ a_k^{(n)}[\cos(k\theta-\varphi)+\cos(k\theta+\varphi)]. \quad (2)$$

On using mechanical similarity for x^{2n}-type potentials [9], the coefficients $a_k^{(n)}$ in (2) scale with action as

$$a_k^{(n)}=\gamma_k^{(n)}I^{1/(n+1)}, \quad (3)$$

having the same exponent for all k, while the constants $\gamma_k^{(n)}$ fall off rapidly with k. Therefore, for our purposes, we shall truncate the series in (2), i.e., approximate

$$H\approx H_0(I)-\epsilon a_1^{(n)}[\cos(\theta-\varphi)+\cos(\theta+\varphi)]. \quad (4)$$

This yields the following evolution equations

$$dI/dt=-\epsilon a_1^{(n)}[\sin\Phi+\sin(\Phi+2\varphi)], \quad (5)$$

$$d\Phi/dt=\Omega_0(I)-\omega(t)+O(\epsilon),$$

where $\Phi\equiv\theta-\varphi$ is the phase mismatch, and $\Omega_0\equiv dH_0/dI=[2n/(n+1)]b_nI^{(n-1)/(n+1)}$ is the frequency of the unperturbed oscillator. The second equation in (5) shows that if one starts out of resonance, i.e., when the difference $\Omega_0(I)-\omega(t_0)$ is positive and larger than the $O(\epsilon)$ term in this equation and $\omega(t)$ slowly increases in time, then the phase mismatch Φ *increases* monotonically in time until $\Omega_0(I)-\omega(t)$ becomes of $O(\epsilon)$. We shall see below that, at certain conditions, beyond this time $\Omega_0(I)-\omega(t)$ remains of $O(\epsilon)$, meaning that the system remains phase locked [$d\Phi/dt=O(\epsilon)$]. When this is the case, one can make an additional approximation and leave only the slowest term in the perturbation in (4), i.e., consider the dynamics described by the approximate, *single resonance* Hamiltonian [10]

$$H''(I,\theta,t)=H_0(I)-\epsilon a_1(I)\cos\Phi. \quad (6)$$

The evolution equations given by this Hamiltonian are

$$\frac{dI}{dt}=-\epsilon a_1\sin\Phi,$$
$$\frac{d\Phi}{dt}=\Omega_0-\omega-\epsilon(da_1/dI)\cos\Phi. \quad (7)$$

Equations (7) differ from those describing the usual nonlinear resonance [10] by the slow time variation of the driving frequency $\omega(t)$. At this stage, we can also include the nearly parabolic potential case within the same system (7), where, for small I, $\Omega_0(I)\approx b_1+2c_1I$ (with constant c_1), while $a_1\approx\gamma_1I^{1/2}$, i.e., has the form (3) with $n=1$. Thus, all cases ($n=1,2,\ldots$) of LPTR can be treated within the same system

$$dI/dt=-\epsilon\gamma_nI^{r_n}\sin\Phi,$$
$$d\Phi/dt=(q_n+1)c_nI^{q_n}-\alpha t-\epsilon r_n\gamma_nI^{-nr_n}\cos\Phi, \quad (8)$$

where, for $n=1$, we have shifted the time to remove the constant term in the right-hand side (RHS) in the second equation in (7); $r_n=1/(n+1)$, $q_n=(n-1)r_n$, $c_n\equiv b_n$ for $n>1$, and $q_n=1$ for $n=1$. Note that (8) comprises a Hamiltonian system for the canonical pair (I,Φ) with the effective Hamiltonian of form

$$H_{eff}=c_nI^{q_n+1}-\alpha tI-\epsilon\gamma_nI^{r_n}\cos\Phi. \quad (9)$$

Now, for definiteness, we focus on the $n=2$ case, i.e., $V=\frac{1}{4}x^4$, for which (8) becomes

$$dI/dt=-\epsilon\gamma_2I^{1/3}\sin\Phi,$$
$$d\Phi/dt=(4/3)c_2I^{1/3}-\alpha t-(\epsilon\gamma_2/3)I^{-2/3}\cos\Phi. \quad (10)$$

First, we present numerical solutions in our system in terms of the action-angle variables in the same example as in Figs. 1(a) and 1(b). These results are shown in Fig. 2(a), where we again used parameters $\epsilon=0.11$, $\alpha=0.005$. The initial conditions were $I=0.15,\theta=3\pi/2$ (at $t_0=10$), while $c_2=0.867$ and $\gamma_2=0.652$ in the $n=2$ case. The calculations were performed in two stages. In the first stage, for $t_0<t<t_s=75$, we used evolution equations based on the two-term approximation of the driving term [(5)], while, for $t>t_s$, switched to the single resonance representation [i.e., to Eqs. (7)]. One can see in the figure that the phase locking in the system starts at $t\approx85$ and continues at later times as the action I increases automatically to satisfy the approximate resonance condition $(4/3)c_2I^{1/3}-\alpha t\approx0$. The latter statement is illustrated by adding the thick line in Fig. 2(a), which shows the function $(3\alpha t/4c_2)^3$ representing the exact resonance. The degree of accuracy of our approximations is illustrated in Fig. 2(b). The figure compares the time dependence of the energy H' (the thin line) found by using (4) where one sub-

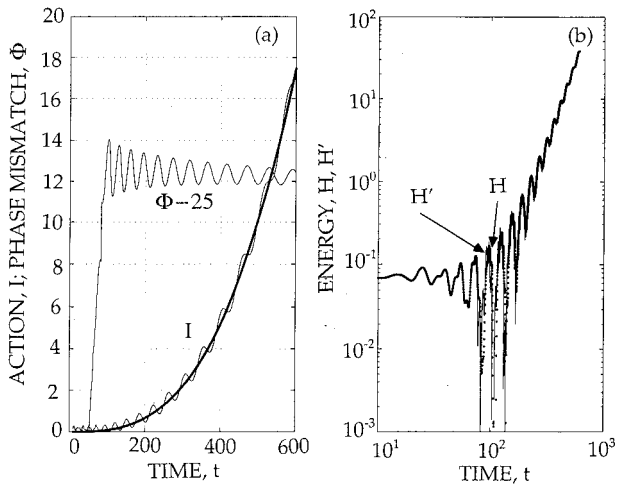

FIG. 2. Autoresonance in two- and (beyond $t_s=75$) single-resonance approximations. (a) The evolution of the action I and phase mismatch Φ. The thick line represents the exact resonance condition; (b) the energy in the system versus time. H is the solution of the exact evolution equations; H' (the thin line) is calculated by using the results shown in (a) substituted in the approximation (5).

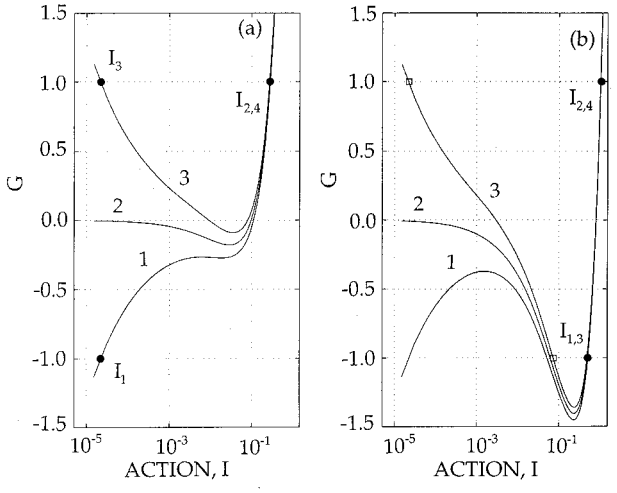

FIG. 3. The auxiliary function $G=\cos\Phi$ versus action I for fixed ω and H_{eff} just above zero (curves 1), $H_{eff}=0$ (curves 2), and H_{eff} just below zero (curves 3). (a) The phase trapping scenario: the minimum of G is above the value of -1 when it occurs first. The full circle dots show the bounds of variation of the action just before and after the phase locking; (b) the minimum of G is below -1 when H_{eff} passes zero. There exists some initial phase mismatch, such that there is no phase trapping in this case. The final state of the system after passage through resonance is within the bounds shown by square dots.

stitutes the data shown in Fig. 1(a) and compares it with H [see (1)] calculated by using the numerical solution of the original evolution equations. We can see in this figure that for $t_0<t<75$ the agreement is excellent, while for $t>75$, when we switch to the single resonance approximation, continues to be very good.

At this stage we proceed to the question of how the phase locking starts in our system. One can answer this question by viewing $\omega(t)=\alpha t$ in the Hamiltonian H_{eff} [see (9)] as a *slowly varying* parameter. If this parameter would be fixed, the energy H_{eff} would be conserved. The phase space portrait of the system in this case can be analyzed by rewriting (9) (for $n=2$ case) as

$$G(I)\equiv\cos\Phi=(\varepsilon\gamma_2)^{-1}\left(c_2 I-\omega I^{2/3}-\frac{H_{eff}}{I^{1/3}}\right). \qquad (11)$$

By studying the RHS of the last equation one finds that for sufficiently small ω the phase space portrait of the system changes its character depending on whether H_{eff} is positive or negative. This is illustrated in two examples in Figs. 3(a) and 3(b). Figure 3(a) shows $G=G(I)$ for $\omega=0.4$, $\varepsilon=0.11$ and three values $H_{eff}=-2\times10^{-3},0,2\times10^{-3}$ (curves 1,2 and 3, respectively). We can see from the figure that for $H_{eff}=2\times10^{-3}$ the phase mismatch Φ grows monotonically $[-1\leqslant\cos\Phi\leqslant+1]$, while the action oscillates in the interval $I_1\leqslant I\leqslant I_2$ (between the corresponding full circle dots in the figure). In contrast, for $H_{eff}=-2\times10^{-3}$ the phase mismatch is bounded and $\cos\Phi$ oscillates between $+1$ and $\cos(\Delta\Phi)$, i.e., $\Phi(\mathrm{mod}\,2\pi)$ oscillates between $\pm\Delta\Phi$, while the oscillations of the action remain in nearly the same limits $I_3\leqslant I\leqslant I_4$. Figure 3(b) presents the same case as Fig. 3(a), but for a larger value of $\omega=0.8$. One can see that in contrast to Fig. 3(a), the minimum of $G(I)$ at $H_{eff}=0$ now lies below -1. Consequently, when one slowly passes from small positive to small negative values of H_{eff}, the system remains detrapped, while the action oscillates in almost the same interval $I_1\approx I_3\leqslant I\leqslant I_4\approx I_2$. We shall see below that, at later times in this case, the minimum value of G increases until it passes the value of -1, while, later, for some initial values of Φ, G decreases again, after the quasi-particle passes to the second detrapped region [denoted by two square dots in Fig. 3(b)].

Now we return to our real system, where the parameter $\omega(t)=\alpha t$ is a slowly varying function of time. In this case H_{eff} also is a slow function of time. Since

$$dH_{eff}/dt=-\alpha I, \qquad (12)$$

H_{eff} *decreases* monotonically. As a result, if one starts at a positive value of H_{eff} and the rate of change of H_{eff} is sufficiently slow (i.e., for sufficiently small α), on the basis of the discussion above, we expect phase trapping to occur at the time when H_{eff} passes zero, provided that the minimum of $G(I)$ at this time is above -1. Note that this argument is independent of the initial value of the phase mismatch and, therefore, the initial positiveness of H_{eff} and the first occurrence of the minimum in $G(I)$ above -1 are the necessary conditions for phase trapping in the system. We demonstrate these conclusions in Fig. 4(a) showing the evolution of the phase mismatch Φ and of H_{eff} in the example presented earlier in Fig. 1. As expected, phase trapping occurs at the moment when H_{eff} passes zero. In contrast, In Fig. 4(b), we start with a larger initial value of the action, $I=0.46$ (larger initial energy) and switch to the single resonance approximation [Eqs. (11)] at later time, $t_s=120$. Here, the minimum of G is less than -1 when it appears first during the evolution and, consequently, there is no phase trapping in this case. Finally, we estimate the phase trapping time. The latter de-

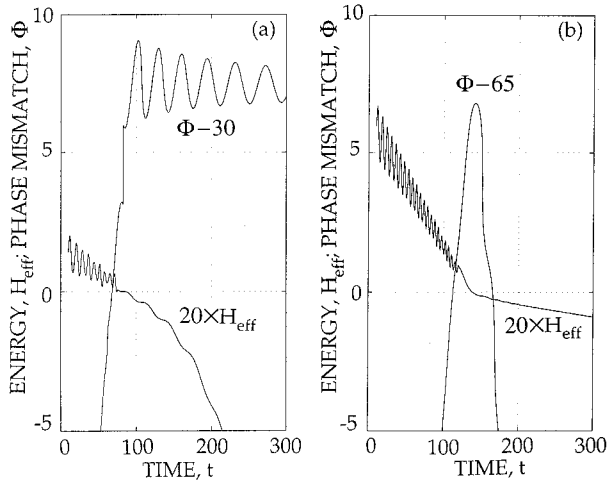

FIG. 4. The energy H_{eff} and phase mismatch Φ versus time in passage through resonance. (a) Sufficiently small and positive initial H_{eff}. The minimum of G occurs first above -1. The phase trapping proceeds as H_{eff} passes zero. (b) Larger initial energy. The minimum of G occurs first below -1 and there is no phase trapping in this case.

pends on initial conditions and can be found by using the *adiabatic invariant* in the problem, i.e.,

$$J(H_{eff},\omega)\equiv(2\pi)^{-1}\int_0^{2\pi} I^* d\Phi \approx \text{const}, \tag{13}$$

where $I^*=I^*(H_{eff},\omega,\Phi)$ is the solution of (11) for I. We illustrate the invariance of J in Fig. 5, showing the (I,Φ) portrait of evolution in the system passing from the detrapped to trapped autoresonant state. We used the same initial conditions and parameters as in Figs. 1 and 2, but $\alpha=0.001$ and $t_s=275$. The invariance of J is seen in the figure as the preservation of the areas $A_{1,2,3}$ inside the parts of the portrait shown by thick lines and corresponding to single

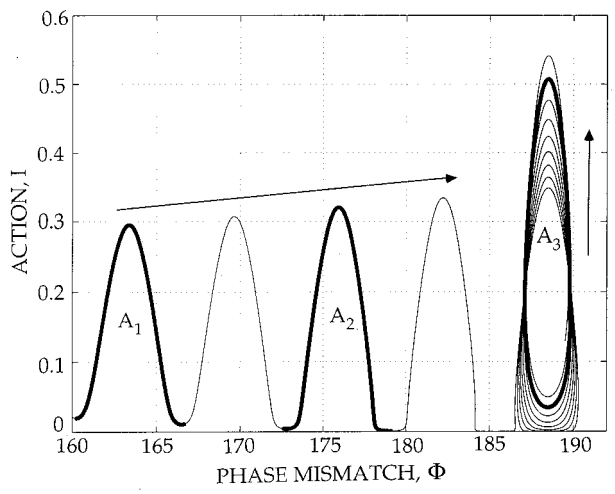

FIG. 5. Action versus phase mismatch during phase trapping via passage through resonance. The conservation of the areas A_i in the figure illustrates the adiabatic invariance of $J=(2\pi)^{-1}\oint I^* d\Phi$ during the evolution from the detrapped (areas $A_{1,2}$) to trapped (area A_3) state of the system. The arrows show the direction of the time evolution of the system.

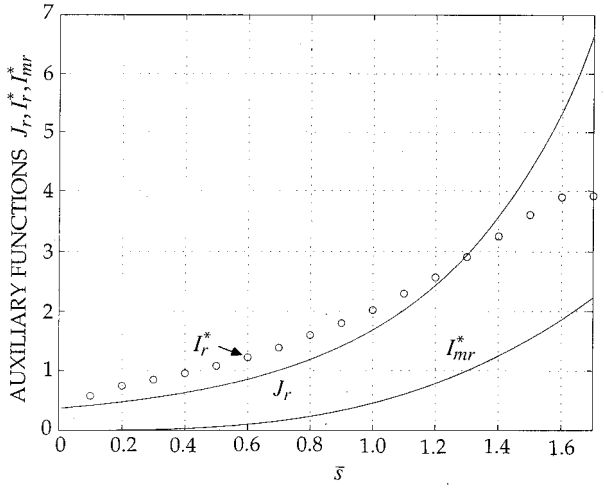

FIG. 6. Auxiliary functions J_r, I_r^* (circles) and I_{mr}^* versus $\bar{s}=\bar{\alpha}t_r$. The function J_r allows to find the phase locking time t_r from initial conditions, while, since $I_r^*>I_{mr}^*$, the amplitude of the phase mismatch oscillations decreases for $t>t_r$.

oscillation periods at different times before (areas $A_{1,2}$) and after (areas A_3) the trapping. Now, if at $t=t_0$, $J=J_0$, and since $\omega=\alpha t$, the expected trapping time t_r is given by $J_r\equiv J(0,\alpha t_r)=J_0$. In addition to $J_r(s)$ (s being defined as $s\equiv\alpha t_r$), additional two *universal* functions evaluated at $H_{eff}=0$ are important in studying the evolution of the system beyond the trapping point (see below). The first is the value of I^* averaged over an oscillation, i.e.,

$$I_r^*(s)\equiv T^{-1}\int_0^T I^* dt, \tag{14}$$

where one averages over the period of oscillation $T(s)=(\partial J/\partial H_{eff})^{-1}$ of the system for fixed values of $H_{eff}=0$ and $\omega=s$. The second function, denoted by $I_{mr}^*(s)$, is the value of I^* at which the function G [see (11)] at $H_{eff}=0$ and $\omega=s$ has a minimum (recall that for trapping this minimum must lie above -1). As defined, the three functions, $J_r(s)$, $I_r^*(s)$, and $I_{mr}^*(s)$, depend on two parameters, ε and α. Nonetheless, the renormalized functions $\bar{J}_r=(\epsilon\gamma_2)^{-1}J_r$, $\bar{I}_r^*=(\epsilon\gamma_2)^{-1}I_r^*$, and $\bar{I}_{mr}^*=(\epsilon\gamma_2)^{-1}I_{mr}^*$ depend on a *single* parameter $\bar{\alpha}=(\epsilon\gamma_2)^{-1/3}\alpha$, via the renormalized variable $\bar{s}=\bar{\alpha}t_r$. We have calculated $\bar{J}_r(\bar{s})$, $\bar{I}_r^*(\bar{s})$, and $\bar{I}_{mr}^*(\bar{s})$ numerically and show these functions in Fig. 6. As described earlier, $\bar{J}_r(\bar{s})$ allows to find the trapping time t_r. On the other hand, we observe in the figure that $\bar{I}_r^*(\bar{s})>\bar{I}_{mr}^*(\bar{s})$. This leads to the conclusion that, after the trapping, the minimum value of G ($=\cos\Phi$) increases towards $+1$, i.e., the amplitude $\Delta\Phi=\cos^{-1}(\min G)$ of the trapped oscillations of the phase mismatch around $\Phi=0 \pmod{2\pi}$ decreases. To prove this statement, we denote $\min G=G(I_{mr}^*)\equiv G^*$ and, by direct differentiation in the vicinity of the trapping point, obtain $dG^*/dt=(\partial G^*/\partial H_{eff})(dH_{eff}/dt)+\partial G^*/\partial t$, or, on using (12),

$$dG^*/dt=(\alpha/\varepsilon\gamma_2)(I_{mr}^*)^{-1/3}(I-I_{mr}^*). \tag{15}$$

This equation shows that G^* increases monotonically if $I - I^*_{mr}$ is positive, as in the detrapped region between the full circle dots in Fig. 3(b). Similarly, G^* decreases monotonically when the particle is in the second detrapped region [between two square in Fig. 3(b)]. The transition between these two types of evolution corresponds to the case when, for some initial Φ, the particle passes from one detrapped region to another and, thus, remains detrapped after passing through resonance. In contrast, if the particle is trapped (either initially, or when G^* appears first above -1), I oscillates around I^*_{mr} and so does G^*, according to (15). At the same time, we find that, in averaging over a single oscillation,

$$d\langle G^*\rangle/dt \approx (\alpha/\varepsilon\gamma_2)(I^*_{mr})^{-1/3}(I^*_r - I^*_{mr}) > 0, \qquad (16)$$

i.e., indeed, the amplitude $\Delta\Phi$ of the system phase mismatch oscillations decreases after the trapping. Similarly, one shows that

$$d\langle I^*_{mr}\rangle/dt \approx (\alpha/3G'')(I^*_{mr})^{-4/3}(I^*_r + 2I^*_{mr}), \qquad (17)$$

where $G''>0$ is the second derivative of G at the minimum. Thus, the minimal action value increases after the trapping. When $\langle I^*_{mr}\rangle$ grows and the amplitude $\Delta\Phi$ of the mismatch oscillations becomes sufficiently small (say $\Delta\Phi < \pi/6$ for definiteness), the systems enters the advanced autoresonant evolution stage, which we consider in the following section.

III. ADVANCED AUTORESONANT EVOLUTION

At this point we assume that during the phase locking process described above, one reaches a stage, where $\Phi(\mathrm{mod}\,2\pi) < \pi/6$, i.e., one can replace $\cos\Phi \approx 1$ in the second equation in (10), yielding a simplified system:

$$dI/dt = -\varepsilon\gamma_2 I^{1/3}\sin\Phi, \qquad (18)$$

$$d\Phi/dt = (4/3)c_2 I^{1/3} - \alpha t - (\varepsilon\gamma_2/3)I^{-2/3}.$$

Then, we seek solutions of (18) in the form $I = \tilde{I} + \delta I$ and $\Phi = \tilde{\Phi} + \delta\Phi$, where $\tilde{I}$ and $\tilde{\Phi}$ are defined by

$$(4/3)c_2\tilde{I}^{1/3} - \alpha t - (\varepsilon\gamma_2/3)\tilde{I}^{-2/3} = 0,$$
$$-\frac{\alpha}{R} - \varepsilon\gamma_2\tilde{I}^{1/3}\sin\tilde{\Phi} = 0, \qquad (19)$$

where

$$R \equiv \alpha(d\tilde{I}/dt)^{-1} = (4/9)c_2\tilde{I}^{-2/3} + (2/9)\varepsilon\gamma_2\tilde{I}^{-5/3}. \qquad (20)$$

Note that $\tilde{\Phi}$ can be defined this way only if $\varepsilon\gamma_2\tilde{I}^{1/3} > \alpha/R$. Furthermore, both $\tilde{I}$ and R are varying monotonically with t ($\tilde{I}$ grows, while R decreases). Now, by assuming that $|\delta I| \ll \tilde{I}$ and $|\delta\Phi| \ll \pi$, we linearize in (18), yielding

$$d(\delta I)/dt = -\varepsilon\gamma_2\tilde{I}^{1/3}\delta\Phi, \qquad (21)$$

$$d(\delta\Phi)/dt = R\,\delta I$$

Equations (21) comprise a Hamiltonian system with the Hamiltonian

$$\delta H = \frac{1}{2}R(\delta I)^2 + \frac{1}{2}\varepsilon\gamma_2\tilde{I}^{1/3}(\delta\Phi)^2, \qquad (22)$$

which describes linear oscillations of $\delta\Phi$ and δI with a slowly varying frequency $\nu = (\varepsilon\gamma_2\tilde{I}^{1/3}R)^{1/2}$. We observe that if $\delta\Phi_{\max}$ and $\delta I_{\max}$ are the amplitudes of these oscillations, then the product $(\delta\Phi)_{\max}\ (\delta I)_{\max}$ is an adiabatic invariant as long as $\nu^{-2}|d\nu/dt| \ll 1$. Therefore, since from (21), $\nu\delta I_{\max} = \varepsilon\gamma_2\tilde{I}^{1/3}\delta\Phi_{\max}$, we have $(\delta I_{\max})^2 \propto R^{-1/2}\tilde{I}^{1/6}$, so $\delta I_{\max}/\tilde{I} \propto R^{-1/4}\tilde{I}^{-11/12}$. Similarly, $\delta\Phi_{\max} \propto R^{1/4}\tilde{I}^{-1/12}$. These results show that both $\delta I_{\max}/\tilde{I}$ and $\delta\Phi_{\max}$ *decrease* with time under adiabatic conditions and, therefore, the adiabaticity condition $\nu^{-2}|d\nu/dt| \ll 1$ is sufficient for sustaining the autoresonance beyond the trapping stage. Let us discuss this condition in more detail. After some algebra, we find

$$\nu^{-2}|d\nu/dt| < C[\tilde{I}^{-1/6} + 2(\varepsilon\gamma_2/c_2)\tilde{I}^{-7/6}], \qquad (23)$$

where $C = (9/16)[\alpha/(\varepsilon\gamma_2)^2](\varepsilon\gamma_2/c_2)^{3/2}$. Since the right hand side in (23) decreases in time, sufficiently small value of α guarantees satisfaction of the adiabaticity condition at all times. Finally, in order to have a slowly varying quasi-steady state defined in (19) one must have $\varepsilon\gamma_2\tilde{I}^{1/3} > \alpha/R$ or

$$\alpha(\varepsilon\gamma_2 R\tilde{I}^{1/3})^{-1} < 1. \qquad (24)$$

This condition brakes for t large enough since $R\tilde{I}^{1/3}$ decreases with time. One can get a good estimate for the braking time t_b by assuming $\tilde{I}_b = \tilde{I}(t_b) \gg 1$. In this case $R\tilde{I}^{1/3} \approx (16/27)c_2^2(\alpha t)^{-1}$ and, therefore,

$$t_b \approx (16/27)(\varepsilon\gamma_2)(c_2/\alpha)^2. \qquad (25)$$

We see that t_b and, consequently, the maximum amplitude of autoresonantly excited oscillator can be controlled by varying the rate of variation α of the driving frequency. Note also that since $\tilde{I}_b \approx (4\varepsilon\gamma_2 c_2/9\alpha)^3$, our assumption $\tilde{I} \gg 1$ is valid for α small enough.

We illustrate our predictions in Fig. 7 showing the autoresonant evolution (solid lines) of $(\Phi+\pi)(\mathrm{mod}\,2\pi) - \pi$ (Fig. 7a) and I (Fig. 7b) for the same parameters and initial conditions as in Fig. 2, but for longer times when the braking of the autoresonance is achieved. The dashed lines in the figures represent $\tilde{\Phi}$ and $\tilde{I}$ respectively. One can see that, as expected, the amplitude of the autoresonant phase oscillations decreases in time and that the autoresonance discontinues at $t \approx 1300$, in an excellent agreement with $t_b = 1278$ from (25) for this case.

IV. CONCLUSIONS

We have studied the problem of trapping into resonance and subsequent autoresonant evolution of a nonlinear oscillator characterized by x^4-type potential and driven by a chirped frequency perturbation. We have shown that, under certain conditions, when the driving frequency increases and passes that of the unperturbed oscillator, the oscillator phase

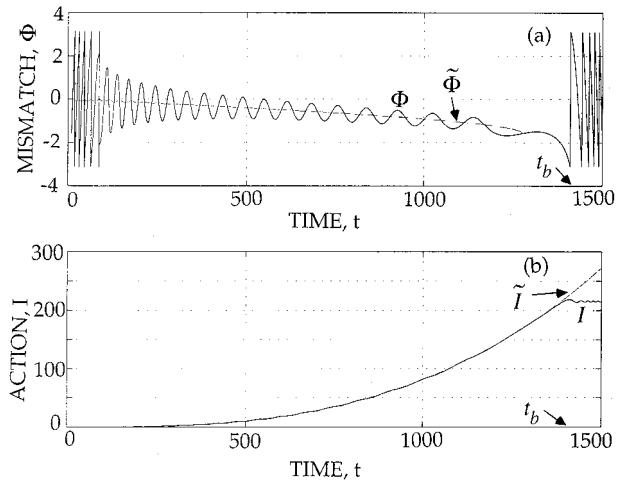

FIG. 7. Evolution of the phase mismatch $(\Phi+\pi)(\mathrm{mod}\,2\pi)-\pi$ [(a)] and the action I [(b)] in the advanced autoresonance stage. The curves $\tilde{\Phi}$ and $\tilde{I}$ represent the quasi-steady-state associated with the autoresonance. The phase locking discontinues at $t\approx t_b$ [see Eq. (25)] as the quasi-steady state ceases to exist.

locks to the drive, and, at later times, the oscillator frequency follows (in average) that of the driving oscillation. This means that a continuing excitation of the system to higher energies takes place, until times scaling as $t_b\sim\alpha^{-2}$ [see (24)] for linearly chirped driving frequency (α being the frequency chirp rate). This time limit can be removed if one gradually reduces the chirp rate as the oscillation amplitude increases in autoresonance. Generalization to x^{2n} $(n>2)$ case can be performed along the same lines as described in Secs. II and III. For example, in studying the trapping stage in the general case, one deals with the characteristic function [compare to (11) for the $n=2$ case]

$$G_n(I)=(\varepsilon\gamma_n)^{-1}\left(c_n I^{\frac{2n-1}{n+1}}-\omega I^{\frac{n}{n+1}}-\frac{H_{eff}}{I^{\frac{1}{n+1}}}\right), \qquad (26)$$

which for different values of H_{eff} has the form similar to that shown in Fig. 3 in the $n=2$ case. We again conclude that for all $n<+\infty$, the trapping takes place when the slowly decreasing H_{eff} (in the general case we also have $dH_{eff}/dt=-\alpha I$) becomes negative, provided that the minimal value of $G_n(I)$ is above -1 when it occurs first in the evolution process. This guarantees phase trapping in the system independently of the initial phase of the oscillator. In contrast, for $n=\infty$ (the square potential well) the last term in the parentheses in the RHS of (26) is simply H_{eff} and there exist no singularity of type $G_n(I)\to-\infty$ at $I\to 0$ at positive values of H_{eff} as in Fig. 3, which is necessary for the appearance of a minimum of $G_n(I)$ *above* the value of -1 at later times after starting in the detrapped state, where this minimum does not exist. Since this is the only scenario for adiabatic transition to the trapped state in our system independently of initial phase, the adiabatic passage through resonance does not lead to automatic phase locking of an adiabatically driven particle in a square potential well. Returning to arbitrary, but finite values of n, as in the $n=2$ case, after the trapping, the system enters the autoresonant evolution stage. Autoresonance continues as long as one satisfies the adiabaticity condition [compare to (23) for the $n=2$ case]

$$\frac{1}{\nu^2}\left|\frac{d\nu}{dt}\right|<C_n\left[\frac{1}{\tilde{I}^{(n-3/2)r_n}}+\frac{n\varepsilon\gamma_n/(n-1)}{c_n\tilde{I}^{(3n-5/2)r_n}}\right], \qquad (27)$$

where $C_n=(\alpha/2)(n+1)^2[2n(n-1)c_n]^{-3/2}(\varepsilon\gamma_n)^{-1/2}$. In addition to (27) one must also satisfy the condition similar to (24)

$$\alpha/(\varepsilon\gamma_n R_n\tilde{I}^{r_n})<1, \qquad (28)$$

where $R_n=[2n(n-1)/(n+1)^2]c_n\tilde{I}^{q_n-1}+nr_n^2\varepsilon\gamma_2\tilde{I}^{-nr_n-1}$. This condition guarantees the existence of a slow quasi-steady state in the system during the advanced autoresonance stage. As in the $n=2$ case, (28) is not satisfied for all times, but is broken at [compare to (25)]

$$t_b=\left[\frac{2n(n-1)c_n\varepsilon\gamma_n}{\alpha(n+1)^2}\right]^n\left[\frac{n+1}{\varepsilon\gamma_n(n-1)}\right]. \qquad (29)$$

Equation (29) shows that, in the limit of large n, for α fixed and small enough, the autoresonance lasts for longer times for larger values of n.

In addition to these applications, we plan to extend our theory to the problem of sub- and higher harmonic autoresonance, as well as to higher dimensional dynamical systems of a similar type. Another interesting direction for future studies is the autoresonance in driven nonlinear wave systems which can be associated with the dynamical problem in x^{2n}-type potentials. One such example is the driven nonlinear Schrodinger equation with higher order nonlinearity [11] $i\psi_t+\psi_{xx}+|\psi|^{2n}\psi=f$. The time independent limit of this equation for real ψ corresponds to the dynamical problem considered in this work.

ACKNOWLEDGMENT

This work was supported by the Israel Science Foundation founded by the Israel Academy of Sciences and Humanities.

[1] M.S. Livingstone, *High Energy Accelerators* (Interscience, New York, 1954).

[2] B. Meerson and L. Friedland, Phys. Rev. A **41**, 5233 (1989); W. K. Liu and B. Wu, Phys. Rev. Lett. **75**, 1292 (1995).

[3] G. Cohen and B. Meerson, Phys. Rev. E **47**, 967 (1992); S. Yariv and L. Friedland, Phys. Rev. E **48**, 3072 (1993).

[4] I. Aranson, B. Meerson, and T. Tajima, Phys. Rev. A **45**, 7501 (1992); L. Friedland and A.G. Shagalov, Phys. Rev. Lett. **81**, 4357 (1998).

[5] L. Friedland, Phys. Rev. E **59**, 4106 (1999).

[6] M. Deutsch, J.E. Golub, and B. Meerson, Phys. Fluids B **3**, 1773 (1991); J. Fajans, E. Gilson, and L. Friedland, Phys. Rev. Lett. **82**, 4444 (1999).

[7] L. Friedland, Phys. Fluids B **4**, 3199 (1992).

[8] L.D. Landau and E.M. Lifshitz, *Mechanics* (Pergamon Press, Oxford, 1969) p. 27.
[9] L.D. Landau and E.M. Lifshitz, *Mechanics* (Ref. [8]), p. 22.
[10] R.Z. Sagdeev, D.U. Usikov, and G.M. Zaslavsky, *Nonlinear Physics: From Pendulum to Chaos* (Harwood, New York, 1988), p. 117.
[11] V.I. Karpman and A.G. Shagalov, Phys. Lett. A **228**, 59 (1997) and references therein.